Growth of Mixed Nonionic Micelles

Henry G. Thomas,† Aleksey Lomakin,† Daniel Blankschtein,*,‡ and George B. Benedek*,†

Department of Physics, Department of Chemical Engineering, and Center for Materials Science and Engineering, Massachusetts Institute of Technology, Cambridge, Massachusetts 02139

Received July 5, 1996. In Final Form: October 29, 1996⊗

Static and quasielastic light-scattering measurements were utilized to investigate the shape, size, and polydispersity of mixed micelles composed of the nonionic surfactants dodecyl hexaoxyethylene glycol monoether ($C_{12}E_6$) and dodecyl octaoxyethylene glycol monoether ($C_{12}E_8$) in aqueous solutions. We determined the molecular weight and diffusion coefficient of these micelles and showed that they are rodlike. The average diffusion coefficient of the mixed micelles was measured at various total surfactant concentrations in the range between approximately 30 and 1000 times the critical micellar concentration of the surfactant mixture. Pure $C_{12}E_6$, pure $C_{12}E_8$, and three different mixtures of $C_{12}E_6$ and $C_{12}E_8$ were studied in the temperature range $10\ °C \leq T \leq 55\ °C$. We found that the mixed micelles could be satisfactorally described as prolate ellipsoids with an average long axis which grows in size as the total surfactant concentration increases. The extent of this growth is more pronounced when the relative proportion of $C_{12}E_6$ in solution is increased or as the temperature approaches the boundary of phase transition into coexisting micelle-rich and micelle-poor phases. We propose a phenomenological model to quantitatively describe the linear growth of rodlike mixed micelles. Two parameters of this model which control the observed linear growth of the mixed $C_{12}E_6$ and $C_{12}E_8$ micelles were deduced from the experimental data and compared with the values predicted by a recently developed molecular−thermodynamic theory of mixed micellization.

I. Introduction

Surfactants are used in a wide variety of industrial and commercial applications. They are exploited for their detergency, solubilization, and surface-wetting capabilities in such diverse areas as the mining, petroleum, chemical, and pharmaceutical industries, as well as in biochemical and medical research. In order to tailor the properties of the surfactant solution to best suit the desired application, one must be able to predict and manipulate (i) the tendency of the surfactant solution to form micelles as reflected by the critical micellar concentration, cmc, (ii) the shape and size distribution of the micelles that form above the cmc, and (iii) the phase behavior of the surfactant solution. Indeed, the concentration of surfactant in a solution, which is used as a cleaning detergent, should exceed the cmc to ensure the presence of micelles in which oily substances or dirt can be solubilized. The shape and size of micelles is directly related to the viscosity and other rheological features of the micellar solution, which are important in many applications involving surfactants, for example, in personal care products.[1] The phase separation phenomenon, which is to be avoided in most practical situations, may be exploited for the separation and purification of macromolecules, such as synthetically produced proteins.[2] Mixtures of surfactants offer a very convenient way to optimize the properties of micellar solutions, since by changing solution composition, one can effectively tune the desired feature to the range needed. For example, addition of nonionic surfactant to an ionic surfactant solution may significantly reduce the cmc[3] and may also significantly increase the size of micelles.[4] Clearly, a thorough understanding of the underlying physics and chemistry of mixed surfactant systems is highly desirable.

Much effort has been devoted in recent years to a theoretical understanding of multicomponent surfactant mixtures. Previous investigations have concentrated on describing the composition dependence of the critical micellar concentration[5−10] and on understanding theoretically micellar growth and the distribution of micellar sizes and compositions.[11,12] More recently, an effort has been made to combine such models for mixed micelles with a thermodynamic theory capable of describing the phase behavior and phase separation of the mixed micellar solution. The resulting theory[13−15] has been successfully utilized to predict[16,17] the micellar properties and phase behavior of a variety of surfactant mixtures.

In spite of the wealth of theoretical work on the properties of mixed micellar solutions mentioned above, the experimental data amenable to analysis in terms of these theories is limited mostly to cmc measurements. Although the size and composition distribution of mixed micelles has been discussed,[10,11] no experimental data on

* To whom correspondence should be addressed.

† Department of Physics and Center for Materials Science and Engineering.

‡ Department of Chemical Engineering and Center for Materials Science and Engineering.

⊗ Abstract published in *Advance ACS Abstracts,* January 1, 1997.

(1) Herb, C. A.; Chen, L. B.; Sun, W. M. In *Structure and Flow in Surfactant Solutions*; Herb, C. A., Prud'homme, R. K., Eds.; American Chemical Society: Washington, DC, 1994.

(2) Liu, C.-L.; Nikas, Y. J.; Blankschtein, D. *AIChE J.* **1995**, *41*, 991.

(3) Scamehorn, J. F. In *Phenomena in Mixed Surfactant Systems*; Scamehorn, J. F., Ed.; ACS Symposium Series 311; American Chemical Society: Washington, DC, 1986.

(4) Dubin, P. L.; Principi, J. M.; Smith, B. A.; Fallon, M. A. *J. Colloid Interface Sci.* **1989**, *127*, 558.

(5) Lange, V. H. *Kolloid Z.* **1953**, *96*, 131.

(6) Shinoda, K. *J. Phys. Chem.* **1954**, *58*, 541.

(7) Clint, J. H. *J. Chem. Soc., Faraday Trans. 1* **1975**, *71*, 1327.

(8) Rubingh, D. N. In *Solution Chemistry of Surfactants*; Mittal, K. L., Ed.; Plenum: New York, 1979; Vol. 1, p 337.

(9) Holland, P. M.; Rubingh, D. N. *J. Phys. Chem.* **1983**, *87*, 1984.

(10) Nagarajan, R. *Langmuir* **1985**, *1*, 331.

(11) Ben-Shaul, A.; Rorman, D. H.; Hartland, G. V.; Gelbart, W. M. *J. Phys. Chem.* **1986**, *90*, 5277.

(12) Stecker, M. M.; Benedek, G. B. *J. Phys. Chem.* **1984**, *88*, 6519.

(13) Puvvada, S.; Blankschtein, D. *J. Phys. Chem.* **1992**, *96*, 5567.

(14) Puvvada, S.; Blankschtein, D. *J. Phys. Chem.* **1992**, *96*, 5579.

(15) Sarmoria, C.; Puvvada, S.; Blankschtein, D. *Langmuir* **1992**, *8*, 2690.

(16) Zoeller, N.; Shiloach, A.; Blankschtein, D. *CHEMTECH* **1996**, *26*, 24.

(17) Zoeller, N.; Blankschtein, D. *Ind. Eng. Chem. Res.* **1995**, *34*, 4150.

S0743-7463(96)00661-0 CCC: $14.00

this distribution were presented in these works. The detailed theory of Puvvada and Blankschtein[13,14] also relies primarily on measurements of the cmc and the cloud-point curves of the mixed surfactant systems studied. In this paper, we report experimental data on the distribution of sizes of mixed micelles as a function of overall surfactant concentration and surfactant composition obtained by light-scattering measurements on mixtures of similar surfactants.

In our studies, we have examined a system consisting of water and the two nonionic surfactants dodecyl hexaoxyethylene glycol monoether ($C_{12}E_6$) and dodecyl octaoxyethylene glycol monoether ($C_{12}E_8$). Micelles of pure $C_{12}E_6$ are believed to exhibit linear growth into cylindrical structures with increasing concentration of surfactant and temperature.[18−20] Micelles of pure $C_{12}E_8$ also exhibit some growth with increasing concentration and temperature,[20−22] although the extent of the growth is significantly smaller than that observed for $C_{12}E_6$.

Rodlike micellar growth (most notably the growth of sodium dodecyl sulfate micelles in aqueous salt solution) has been explained quantitatively in the context of the phenomenological "ladder model".[23] This model provides a general description of the locally cylindrical micelles in terms of two phenomenological parameters. The first parameter reflects the reduction of the free energy associated with the transfer of a surfactant molecule from a fixed position in solution to a fixed position in the cylindrical region of a micelle. The second parameter reflects the reduction of the free energy per surfactant molecule associated with the formation of two hemispherical end caps. The model also assumes that no micelle can be smaller than the spherical micelle consisting of just the two end caps, referred to as the minimal micelle. The difference in the free energy per surfactant molecule in the end caps and the free energy per surfactant molecule in the cylindrical portion of a micelle controls the extent of micellar growth in the system. The ladder model has been successfully utilized to describe micellar growth in several systems,[23,24] including the $C_{12}E_6$ and water system. Since the ladder model does not account for the interactions between micelles, it is expected to work best for dilute micellar solutions, where intermicellar interactions are negligible. Of course, the overall surfactant concentration should be sufficiently above the cmc so that micellar growth actually occurs. In this paper, we generalize the ladder model for the case of surfactant mixtures.

It should be stressed that both $C_{12}E_6$ and $C_{12}E_8$ aqueous solutions exhibit a lower consolute temperature phase transition from a single isotropic micellar phase into two isotropic micellar phases differing in total surfactant concentration. Reported values for the critical temperature T_C of the $C_{12}E_6$ and water system range from 50.35[25] to 51.3 °C,[26] while T_C values for the $C_{12}E_8$ and water system range from 74.0[22] to 78.4 °C.[14] The corresponding critical concentrations X_C of each surfactant are about 2.3 wt % for $C_{12}E_6$[27] and 3.2 wt % for $C_{12}E_8$.[28] Because of the proximity of the phase boundary, care must be taken in the interpretation of light-scattering data. Specifically, in the close vicinity of the phase boundary and at surfactant concentrations comparable to X_C, correlations between the positions of the interacting micelles become important and may significantly affect the results of the light-scattering measurements. This has led several authors[25,26,29−32] to the conclusion that scattering measurements provide no evidence of micellar growth in the $C_{12}E_6$−water and $C_{12}E_8$−water systems. However, other evidence[18−20] strongly suggests that, even in the vicinity of the critical point, micellar growth is significant. A thorough discussion of these issues can be found in ref 20. In this paper, we report the results of light-scattering experiments conducted in the dilute regime where intermicellar interactions are weak. We have also obtained some data in the high surfactant concentration regime, where the consideration of intermicellar interactions becomes important for the interpretation of our results.

The remainder of the paper is organized as follows. In section II, the sample preparation and the experimental procedures followed in our static and quasielastic light-scattering measurements are discussed. We also briefly discuss the regularization program used for the analysis of the quasielastic light-scattering data. In section III, a generalization of the ladder model to the case of binary mixtures of similar surfactants is presented. The term "similar surfactants" refers here to a surfactant mixture in which the interaction energy per surfactant molecule in the mixed micelle can be obtained as a linear interpolation in composition between the corresponding energies in the pure micelles. In section IV, via a set of combined static and quasielastic light-scattering measurements, we demonstrate that mixed micelles of $C_{12}E_6$ and $C_{12}E_8$ have rodlike structures. We report the dependence of the average hydrodynamic radius of these micelles as a function of surfactant concentration, surfactant composition, and temperature. The generalized "two-dimensional" ladder model is applied to describe our experimental data pertaining to the regions of the phase diagram where intermicellar interactions should be weak. Phenomenological growth parameters of the ladder model deduced from our data are compared with the predictions of a recently developed molecular−thermodynamic theory of mixed micellization.[13,14] Finally, in section V, we present some concluding remarks.

II. Materials and Methods

Sample Preparation. Dodecyl hexaoxyethylene glycol monoether ($C_{12}E_6$, lot 9011, molecular weight 450 Da) and dodecyl octaoxyethylene glycol monoether ($C_{12}E_8$, lot 9054, molecular weight 538 Da) were obtained from Nikko Chemicals, Tokyo, and used as received. Aqueous solutions of the surfactants were prepared by weight using reagent grade water from a Millipore filtration system (Millipore, Bedford, MA) which was first degassed and then saturated with filtered argon. To remove dust, samples were pushed once through a rinsed 0.22 μm

(18) Brown, W.; Johnsen, R.; Stilbs, P.; Lindman, B. *J. Phys. Chem.* **1983**, *87*, 4548.
(19) Ravey, J.-C. *J. Colloid Interface Sci.* **1983**, *94*, 289.
(20) Lindman, B.; Wennerström, H. *J. Phys. Chem.* **1991**, *95*, 6053.
(21) Jonströmer, M.; Jönsson, B.; Lindman, B. *J. Phys. Chem.* **1991**, *95*, 3293.
(22) Kato, T.; Anzai, S.; Takanoi, S.; Seimiya, T. *J. Chem. Soc., Faraday Trans. 1* **1989**, *85*, 2499.
(23) Missel, P. J.; Mazer, N. A.; Benedek, G. B.; Young, C. Y.; Carey, M. C. *J. Phys. Chem.* **1980**, *84*, 1044.
(24) Blankschtein, D.; Thurston, G. M.; Benedek, G. B. *J. Chem. Phys.* **1986**, *85*, 7268.
(25) Corti, M.; Degiorgio, V. *J. Phys. Chem.* **1981**, *85*, 1442.
(26) Wilcoxon, J. P.; Schaefer, D. W.; Kaler, E. W. *J. Chem. Phys.* **1989**, *90*, 1909.
(27) Strey, R.; Pakusch, A. In *Surfactants in Solution*; Mittal, K. L., Bothorel, P., Eds.; Plenum Press: New York, 1986; Vol. 4, p 465.
(28) Degiorgio, V. In *Proceedings of the International School of Physics Enrico Fermi—Physics of Amphiphiles: Micelles, Vesicles and Microemulsions*; Degiorgio, V., Corti, M., Eds.; North-Holland Physics Publishing: Amsterdam, 1985; p 303.
(29) Triolo, R.; Magid, L. J.; Johnson, J. S.; Child, H. R. *J. Phys. Chem.* **1982**, *86*, 3689.
(30) Corti, M.; Minero, C.; Degiorgio, V. *J. Phys. Chem.* **1984**, *88*, 309.
(31) Cantù, L.; Corti, M.; Degiorgio, V.; Minero, C.; Piazza, R. *J. Colloid Interface Sci.* **1985**, *105*, 628.
(32) Zulauf, M.; Weckström, K.; Hayter, J. B.; Degiorgio, V.; Corti, M. *J. Phys. Chem.* **1985**, *89*, 3411.
(33) Brown, W.; Pu, Z.; Rymdén, R. *J. Phys. Chem.* **1988**, *92*, 6086.

Millipore filter (Millex-GV, Millipore, Bedford, MA) and then centrifuged for at least 30 min at 4600*g*. Hereafter, samples will be identified in terms of the total mole fraction X of surfactant contained in the solution and the relative surfactant composition, α_s, which indicates the relative proportion of $C_{12}E_6$ in the mixture. Specifically, in a solution containing N_A moles of $C_{12}E_6$, N_B moles of $C_{12}E_8$, and N_W moles of water, $X = (N_A + N_B)/(N_A + N_B + N_W)$ and $\alpha_s = N_A/(N_A + N_B)$. The critical concentration for phase separation of $C_{12}E_6$, 2.3 wt %, corresponds to $X_C = 9.4 \times 10^{-4}$, and the critical concentration of $C_{12}E_8$, 3.2 wt %, corresponds to $X_C = 1.1 \times 10^{-3}$. Note that the cmc of $C_{12}E_6-C_{12}E_8$ aqueous mixtures is within $(2.0 \pm 0.1) \times 10^{-6}$ for all solution compositions.[14]

Quasielastic Light-Scattering Measurements and Data Analysis. The quasielastic light-scattering (QLS) instruments used in this study are described in detail elsewhere.[23,34,35] All measurements were performed at a scattering angle $\theta = 90°$ using vertically polarized light with a wavelength $\lambda = 488$ nm from an argon ion laser (Coherent Innova 90-5, or Spectra-Physics 164). The photocurrent autocorrelation function was obtained using a Langley-Ford model 1096 correlator (Amherst, MA) with 144 linearly spaced channels.

In QLS, one measures the fluctuations in the light scattered from a solution of particles. In the regime where interparticle interactions are negligible, these fluctuations are caused by the independent Brownian motion of the particles. The contribution of each particle to the scattered light correlation function has an exponential form with a decay rate $\Gamma = Dq^2$, where D is the translational diffusion coefficient and $q = (4\pi n/\lambda)\sin(\theta/2)$ is the scattering vector. The refractive index of water is $n = 1.33$. If all the particles in the solution have the same size, it is a simple task to extract their diffusion coefficient from the measured correlation function. However, in the case of polydisperse systems, the analysis of the correlation function is not as straightforward. The most popular method, the cumulant expansion,[36,37] permits the determination of the average diffusion coefficient and, with less accuracy, the width of the particle distribution. While extremely accurate for narrow distributions, this method yields rather ambiguous results when the size distribution is broad.

In the last decade, powerful alternatives to the cumulant expansion have been developed. These methods[38-40] permit the reconstruction of the distribution of diffusing particles assuming that this distribution is reasonably smooth. Below, we briefly discuss the essentials of the analysis method that we have used.

For a polydisperse system, we may write the normalized homodyne correlation function $g^{(2)}(\tau)$ as

$$g^{(2)}(\tau) = |g(\tau)|^2 + B \tag{1}$$

where B is the baseline, τ is the delay time, and $g(\tau)$ is given by

$$g(\tau) = \int_0^\infty A(\Gamma)\, e^{-\Gamma\tau}\, d\Gamma \tag{2}$$

Our experiment allows us to measure directly the quantity $G(\tau_i) = g^{(2)}(\tau_i) - B$ for a discrete set of delay times $\{\tau_i\}$. In order to determine the distribution of particle diffusion coefficients that fits the data in the best possible way, we need to find $A(\Gamma)$ which minimizes the fourth-order functional

$$\Omega_0(A) = \sum_i (G(\tau_i) - g^2(\tau_i))^2 \tag{3}$$

This functional, $\Omega_0(A)$, is the mean-squared deviation of the measured points $G(\tau_i)$ from the fitting function $g^2(\tau_i)$. Since $A(\Gamma)$ represents the scattering intensity of particles with decay rate Γ, we should apply the physical restriction that $A(\Gamma)$ must be positive or zero when the minimization is performed.

Unfortunately, this minimization problem is ill-posed: small changes in the experimentally measured quantities can result in large, fast oscillating fluctuations in $A(\Gamma)$. However, physically, we expect the particle size distribution to be a smooth function of Γ. To impose this requirement, we add a small stabilization term to $\Omega_0(A)$ and minimize the functional

$$\Omega(A,\delta) = \Omega_0(A) + \gamma \int_0^\infty A^2(\Gamma)\, d\Gamma \tag{4}$$

which favors smooth solutions $A(\Gamma)$. The factor γ in eq 4 is referred to as a regularization parameter. The algorithm utilizes the method of a gradient projections in a series of successive approximations, each quadratic in $A(\Gamma)$. The function $A(\Gamma)$ was computed at 60 logarithmically spaced points with relaxation times ranging from 1 to 256 correlator sample times.

The choice of the regularization parameter γ is important, since it increases the smoothness of the solution at the expense of some systematic distortion. This distortion can be felt as a slight increase in the mean squared deviation Ω_0 from its absolute minimum at $\gamma = 0$. The regularization parameter must therefore be chosen to be as small as possible, yet large enough to make the solution insensitive to the random errors in the experimental measurement. We have chosen a γ that increases Ω_0 from its absolute minimum value at $\gamma = 0$ by approximately 1%. This criterion, although somewhat arbitrary, provides an objective way of choosing γ consistent with the measurement accuracy and the shape of the distribution.

The function $A(\Gamma)$ could be converted into a distribution of the scattering particles over their diffusion coefficient D or over their hydrodynamic radius R_H related to D by the Stokes−Einstein relation

$$D = \frac{k_B T}{6\pi\eta R_H} \tag{5}$$

where k_B is the Boltzmann constant, T is the absolute temperature, and η is the solvent viscosity. The hydrodynamic radius depends on the shape of the particle. For the prolate ellipsoid which we used to model our micelles, the hydrodynamic radius is given by[41]

$$R_H = \frac{b(1 - x^2)^{1/2}}{\ln\left[\dfrac{1 + (1 - x^2)^{1/2}}{x}\right]} \tag{6}$$

where a is the semiminor axis, b is the semimajor axis, and $x = a/b$. Using the regularization procedure, we have found that the measured correlation functions are consistent with a smooth, relatively narrow distribution of micelles which could be sufficiently well characterized by the average diffusion coefficient $\bar{D}$ or apparent hydrodynamic radius $\bar{R}_H$ related to $\bar{D}$ by the same eq 5. We then compared the average quantities $\bar{R}_H$ or $\bar{D}$ with those calculated theoretically, using the size distribution of micelles found from the ladder model. In these calculations, we took the intensity of light scattered by each micelle to be proportional to its squared molecular weight times the structure factor of the corresponding prolate ellipsoid.

We should note that, in our initial studies, when dust removal was accomplished by continuous filtering of the sample through a rinsed 0.22 μm Millipore filter (Millex-GV, Millipore, Bedford, MA) using a peristaltic pump, the distribution of particle sizes obtained from the measured autocorrelation function contained two peaks, as shown in Figure 1b. The leftmost peak corresponds to micelles, while the other peak is consistent with the presence of particles which are an order of magnitude larger in size. Such a bimodal distribution of particle sizes has been observed by others[33] in $C_{12}E_7$ and $C_{12}E_8$ aqueous solutions. However, when dust was removed by centrifugation, the distribution of decay rates contained only a single peak centered around the expected micellar radius, as shown in Figure 1a. We therefore concluded

(34) Mazer, N. A.; Benedek, G. B.; Carey, M. C. *J. Phys. Chem.* **1976**, *80*, 1075.
(35) Chamberlin, R. A. Ph.D. Thesis, Massachusetts Institute of Technology, 1991.
(36) Koppel, D. E. *J. Chem. Phys.* **1972**, *57*, 4814.
(37) Phillies, G. D. J. *J. Chem. Phys.* **1988**, *89*, 91.
(38) Provencher, S. W. *Comput. Phys. Commun.* **1982**, *27*, 213.
(39) Braginskaya, T. G.; Dobitchin, P. D.; Ivanova, M. A.; Klyubin, V. V.; Lomakin, A. V.; Noskin, V. A.; Shmelev, G. E.; Tolpina, S. P. *Phy. Scr.* **1983**, *28*, 73.
(40) Skilling, J.; Bryan, R. K. *Mon. Not. R. Astron. Soc.* **1984**, *211*, 111.
(41) Perrin, F. *J. Phys. Radium* **1936**, *7*, 1.

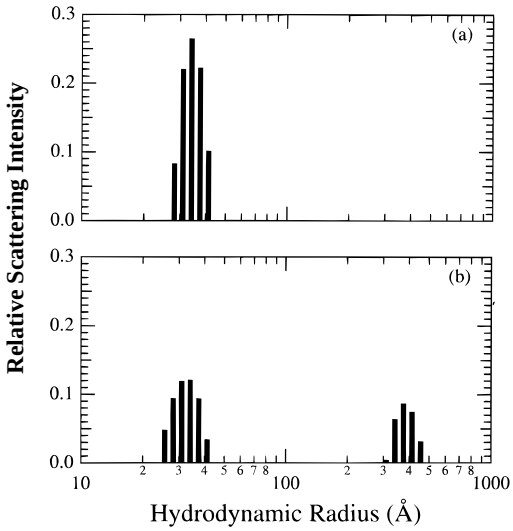

Figure 1. Normalized distribution of particle sizes for a solution of pure $C_{12}E_8$ and water at $T = 25$ °C and $X = 1 \times 10^{-5}$: (a) when samples are prepared by a single filtering step followed by centrifugation; (b) when samples are filtered continuously (see text). The vertical scale is the fractional contribution to the total scattering intensity from particles of the indicated size.

that the filtering process produces big particles, presumably vesicles, and avoided continuous filtering in all subsequent measurements.

Total Intensity Measurements. Total intensity measurements were made using an instrument based on the design of Haller *et al.*[42] which is described in great detail elsewhere.[35] A vertically polarized argon ion laser (Coherent Innova 90-5) operating at $\lambda = 488$ nm was used, and the scattered light was collected at up to 12 fixed angles in the range ($11.5° \leq \theta \leq 162.6°$). Using a procedure described elsewhere,[43,44] we determined the osmotic incompressibility, $\partial\pi/\partial c$, of the micellar solution. The refractive index increment dn/dc was measured using a refractometer (Bausch and Lomb Abbe-3L). Neglecting intermicellar interactions, we calculated the apparent molecular weight of the micelles M_{app} using the following relation[45]

$$\frac{1}{k_B T}\frac{\partial \pi}{\partial c} = \frac{1}{M_{app}} \tag{7}$$

III. Theory

Ladder Model for Single-Component Micelles. For a solution of a single surfactant, the size distribution of micelles of certain shape can be described in terms of the mole fraction X_n of micelles containing n surfactant molecules ($n = 1, 2, 3, ...$). At equilibrium, the distribution of micelles will be such that the chemical potential of a surfactant molecule is identical in all environments. Specifically, if μ_n is the chemical potential of a micelle of total aggregation number n and μ_1 is the chemical potential of a surfactant monomer in solution, then, at equilibrium,[46]

$$\mu_n/n = \mu_1 \tag{8}$$

For dilute solutions, the chemical potentials μ_n and μ_1 are related to the corresponding mole fractions of micelles X_n and free monomers X_1 according to[47]

$$\mu_n = \mu_n^\circ + k_B T \ln X_n \tag{9}$$

$$\mu_1 = \mu_1^\circ + k_B T \ln X_1 \tag{10}$$

where μ_n° and μ_1° are the "standard" parts of the chemical potentials of a micelle of aggregation number n and of a free surfactant molecule, respectively. Substituting eqs 9 and 10 into eq 8, we obtain the equilibrium distribution of micelles in terms of the mole fraction of free surfactant molecules X_1:

$$X_n = {X_1}^n \exp[-(\mu_n^\circ - n\mu_1^\circ)/k_B T] \tag{11}$$

To find the equilibrium micellar distribution for a given total surfactant mole fraction X, one should express X_1 in terms of X using eq 11 and the material conservation condition

$$X = \sum_{n=1}^{\infty} n X_n \tag{12}$$

The first factor in the micellar distribution given by eq 11, ${X_1}^n$, represents the likelihood that n surfactant molecules are localized in the same region of the solution. The second, exponential term is a Boltzmann factor that expresses the reduction of free energy ($\mu_n^\circ - n\mu_1^\circ$) associated with assembling n localized monomers into a micelle (in the absence of intermicellar interactions). Clearly, to fully characterize the micellar system, this free energy of micellization should be known for all n.

The formation of cylindrical micelles, like in aqueous solutions of $C_{12}E_6$ or $C_{12}E_8$, is of particular interest, since the free energy of micellization has a very simple form: it is a linear function of the aggregation number n for large n. Near the cmc, such a system exists as a relatively monodisperse distribution of small spherical or ellipsoidal micelles with some minimum aggregation number $n_0 \gg 1$ in equilibrium with free surfactant molecules. Aggregates with less than n_0 monomers cannot exist because the hydrophilic heads of the constituent surfactant molecules cannot adequately screen the hydrophobic core of the micelle. Far above the cmc, however, long cylindrical micelles are formed and the average size of these micelles increases as the surfactant concentration increases. The "ladder model"[23] was introduced to describe such systems. Each long micelle of total aggregation number n is modeled as a cylindrical body containing $n - n_0$ surfactant molecules and two hemispherical end caps, each containing $n_0/2$ surfactant molecules. The free energy of micellization ($\mu_n^\circ - n\mu_1^\circ$) is modeled as

$$\mu_n^\circ - n\mu_1^\circ = \Delta + (n - n_0)\delta \tag{13}$$

where the parameter Δ is referred to as the "gap spacing" and the parameter δ is referred to as the "rung spacing." According to Tanford,[48] the free energy of micellization per surfactant molecule depends on the cross-sectional area available to the surfactant molecule on the surface of the micelle. This area depends in turn on the local geometry and packing in the micelle. The ladder model, then, postulates that there are two regions of distinct geometry in a micelle, the hemispherical end caps and the cylindrical body. Each of the $n - n_0$ surfactant molecules in the cylindrical body has the same local environment and contributes a quantity δ to the micellization free energy. The n_0 surfactant molecules in the hemispherical end caps contribute a quantity Δ to the

(42) Haller, H. R.; Destor, C.; Cannell, D. S. *Rev. Sci. Instrum.* **1983**, *54*, 973.
(43) Schurtenberger, P.; Chamberlin, R. A.; Thurston, G. M.; Thomson, J. A.; Benedek, G. B. *Phys. Rev. Lett.* **1989**, *63*, 2064.
(44) Thomas, H. G. Ph.D. Thesis, Massachusetts Institute of Technology, 1995.
(45) Debye, P. *J. Phys. Colloid Chem.* **1947**, *51*, 18.
(46) Tanford, C. *The Hydrophobic Effect*; Wiley: New York, 1980.
(47) Israelachvili, J. N.; Mitchel, D. J.; Ninham, B. W. *J. Chem. Soc., Faraday Trans. 2* **1976**, *72*, 1525.
(48) Tanford, C. *J. Phys. Chem.* **1974**, *78*, 2469.
(49) Puvvada, S.; Blankschtein, D. *J. Chem. Phys.* **1990**, *92*, 3710.

micellization free energy. In other words, the quantity Δ is the micellization free energy corresponding to a minimal, spherical micelle containing n_0 surfactant molecules and no cylindrical body. The difference $\Delta - n_0\delta \equiv \Delta\mu$ represents the free energy required to form two end caps in the cylindrical body of the micelle and controls the extent of micellar growth.[23] Elongation is favored when $\Delta\mu > 0$. Substitution of eq 13 in eq 11 results in the following expression for the micellar size distribution:

$$X_n = X_1{}^n \frac{1}{K} e^{-nB} \tag{14}$$

where $B = \delta/k_BT$ and $K = \exp(\Delta\mu/k_BT)$.

Generalization to Multicomponent Micelles. For a solution of two different surfactants containing mixed micelles of well defined geometry, the distribution can be described in terms of the mole fraction $X_{n,\alpha}$ of micelles of composition α, containing n surfactant molecules. The composition variable α runs from 0 to 1, expressing the relative proportion of one of the surfactants in the micelle (in our particular case, $C_{12}E_6$). We shall see shortly that the expressions describing the micellar distribution in the case of mixed micelles are structurally similar to eqs 11 and 13 for single-component micelles. The difference is that the parameters Δ and δ will now be dependent on the micellar composition α and that the mixing entropy of the two surfactant species within the mixed micelle must now be taken into account.

Starting from a general expression for the partition function of the mixed micellar solution and limiting the analysis to the case of a sufficiently dilute solution where intermicellar interactions are negligible, it can be shown that, at equilibrium, the mole fraction of micelles each of which contains n_A surfactant A molecules and n_B surfactant B molecules can be written as[44]

$$X_{n_A,n_B} = \frac{(n_A + n_B)!\, X_{1A}{}^{n_A} X_{1B}{}^{n_B}}{n_A! n_B!} \exp\{-\epsilon(n_A,n_B)/k_BT\} \tag{15}$$

where X_{1A} and X_{1B} are the mole fractions of free surfactant A and free surfactant B monomers, respectively. As in eq 11 for single-component micelles, the factor $X_{1A}{}^{n_A}X_{1B}{}^{n_B}$ in eq 15 represents the likelihood that n_A surfactant A molecules and n_B surfactant B molecules are localized in the same region of the solution, while the combinatorial factor $(n_A + n_B)!/(n_A!n_B!)$ represents the total number of different ways in which these monomers can form a mixed micelle. The exponent is a Boltzmann factor that accounts for the reduction of free energy $\epsilon(n_A,n_B)$ associated with assembling a mixed micelle from these localized monomers.

We can rewrite eq 15 in terms of the total micelle aggregation number $n = n_A + n_B$ and composition $\alpha = n_A/(n_A + n_B)$. Assuming that n_A and n_B are large numbers and using Stirling's approximation, we obtain

$$X_{n,\alpha} = \frac{X_1{}^n}{\sqrt{2\pi n\alpha(1-\alpha)}} \exp\left\{-\left[\epsilon(n,\alpha) + nk_BT\left(\alpha \ln\frac{\alpha}{\alpha_1} + (1-\alpha)\ln\frac{1-\alpha}{1-\alpha_1}\right)\right]/k_BT\right\} \tag{16}$$

where $X_1 = X_{1A} + X_{1B}$ is the total free surfactant monomer mole fraction and $\alpha_1 = X_{1A}/(X_{1A} + X_{1B})$ is the composition of free surfactant monomers in solution. In deriving eq 16, we assumed, for the sake of simplicity, that the composition in the micellar body is the same as that in the micellar ends. The basis for this simplification will be discussed later. The quantity $\epsilon(n,\alpha)$ in eq 16 represents the free energy advantage associated with assembling a mixed micelle of total aggregation number n and composition α from the corresponding surfactant molecules in solution. The second term in the exponent in eq 16 represents the decrease in the mixing entropy of the system upon creating an n-mer of composition α from a mixture of free surfactant monomers having solution composition α_1. Note that this decrease is minimal (zero) when $\alpha = \alpha_1$.

It is essential to keep the multiplicative factors, $\sqrt{2\pi n}$, when using Stirling's approximation for $n!$ in order to obtain a properly normalized micellar distribution function. In principle, the corresponding terms could be added directly to the expression for the free energy of micelle formation, which essentially is the logorithm of the distribution function.[50,51] However, free energy is an extensive quantity, and ln n terms should not be kept in the thermodynamic limit, $n \to \infty$. Since composition itself is defined as a continuous variable only in the limit $n \to \infty$, there is no straightforward way to account for the normalizing factors in the expression for the free energy as a function of n and α. As a result, starting from the chemical potentials, as in the previous section, we would not have been able to recover naturally the correct normalization of the mixed micelle distribution function. This, in turn, as will be explained below, may lead to erroneous conclusions.

To actually find the distribution of micelles using eq 16, one needs to know the micellization free energy $\epsilon(n,\alpha)$ as a function of n and α. For this purpose, we generalize the ladder model to the case of surfactant mixtures by allowing the gap and rung spacings in eq 13 to be functions of micelle composition, that is,

$$\epsilon(n,\alpha) = \Delta(\alpha) + (n - n_0)\delta(\alpha) \tag{17}$$

It is clear that, for $\alpha = 0$ and $\alpha = 1$, $\Delta(\alpha)$ and $\delta(\alpha)$ should reduce to the gap and rung spacings corresponding to pure surfactant A and pure surfactant B solutions, respectively. For the case of similar surfactants, such as $C_{12}E_6$ and $C_{12}E_8$, we take $\Delta(\alpha)$ and $\delta(\alpha)$ to be linear functions of micelle composition α, as shown in Figure 2. We suggest that $\Delta(\alpha) = \alpha\Delta_A + (1-\alpha)\Delta_B$ and that $\delta(\alpha) = \alpha\delta_A + (1-\alpha)\delta_B$, where Δ_A and Δ_B are the gap spacings and δ_A and δ_B are the corresponding rung spacings associated with the single-component micelles of pure surfactant A and pure surfactant B molecules, respectively.

For the formation of micelles to be favored, both $\Delta(\alpha)$ and $\delta(\alpha)$ should be negative quantities. As in the single-component case, the difference $\Delta(\alpha) - n_0\delta(\alpha) \equiv \Delta\mu(\alpha)$ controls the extent of micellar growth. When this difference is negative, end formation is favored and small micelles are formed, while when it is positive, elongation is favored and micellar growth can occur. The quantity $\Delta\mu(\alpha)$ depends on the differences $\Delta\mu_A = \Delta_A - n_0\delta_A$ and $\Delta\mu_B = \Delta_B - n_0\delta_B$ that control the growth of the corresponding single-component micelles, as follows

$$\Delta\mu(\alpha) = \alpha\Delta\mu_A + (1-\alpha)\Delta\mu_B \tag{18}$$

We refer to the two physically meaningful quantities $\Delta\mu_A$ and $\Delta\mu_B$ as growth parameters.

Using the above definitions, the micellar size and composition distribution can be written in the following simple form

(50) Bergstrom, M.; Eriksson, J. C. *Langmuir* **1992**, *8*, 36.
(51) Bergstrom, M. *Langmuir* **1996**, *12*, 2454.

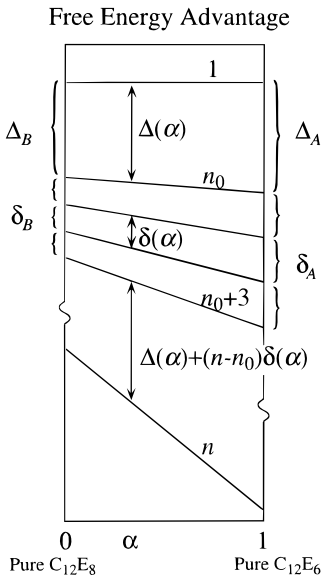

Figure 2. Schematic representation of the two-dimensional ladder model for similar surfactants. The gap spacing $\Delta(\alpha)$ is a linear interpolation in composition between the gap spacing for pure $C_{12}E_8$, Δ_B, and the gap spacing for pure $C_{12}E_6$, Δ_A. The rung spacing $\delta(\alpha)$ is a linear interpolation in composition between the rung spacing for pure $C_{12}E_8$, δ_B, and the rung spacing for pure $C_{12}E_6$, δ_A.

$$X_{n,\alpha} = \frac{{X_1}^n}{\sqrt{2\pi n\alpha(1-\alpha)}} \frac{1}{K(\alpha)} e^{-nB(\alpha)} \tag{19}$$

where $K(\alpha) = \exp\{\Delta\mu(\alpha)/k_BT\}$ and

$$B(\alpha) = \frac{\delta(\alpha)}{k_BT} + \alpha \ln\frac{\alpha}{\alpha_1} + (1-\alpha)\ln\frac{1-\alpha}{1-\alpha_1} \tag{20}$$

The minimum in the quantity $B(\alpha)$ defines the optimal composition of the mixed micelles α^*. According to eq 19, the width of the distribution in composition is proportional to $[nB''(\alpha)]^{-1/2}$. Since n is always a large number ($n \geq n_0$), the micellar distribution $X_{n,\alpha}$ will be very narrowly peaked around α^*. We note also that, if the generalized rung spacing $\delta(\alpha)$ in eq 20 is independent of α, then the minimum in $B(\alpha)$ occurs at $\alpha^* = \alpha_1$. In other words, the optimal micellar composition in this case is the same as the composition of the free surfactant molecules in solution.

To express the micellar distribution given by eq 19 in terms of the total mole fraction X and composition α_s of surfactant in the solution, we use two mass-conservation expressions, one for X and the other for the total mole fraction of surfactant A molecules $\alpha_s X$, namely,

$$X = X_1 + \sum_{n,\alpha} nX_{n,\alpha} \tag{21}$$

$$\alpha_s X = \alpha_1 X_1 + \sum_{n,\alpha} \alpha n X_{n,\alpha} \tag{22}$$

After substitution of eq 16, eqs 21 and 22 can be solved numerically to obtain the mole fraction X_1 and composition α_1 of free surfactant monomers in terms of the total surfactant concentration X and solution composition α_s. In doing so, it is helpful to take into account the fact that the micellar size and composition distribution is narrow in the composition variable α. This permits simplification of the problem by saddle point integration of the mass-conservation relations, eqs 21 and 22, over composition. These equations then become

$$X = X_1 + \sum_{n=n_0}^{\infty} n\tilde{X}_n \tag{23}$$

$$\alpha_s X = \alpha_1 X_1 + \alpha^* \sum_{n=n_0}^{\infty} n\tilde{X}_n \tag{24}$$

with

$$\tilde{X}_n = \frac{{X_1}^n}{K(\alpha^*)} \exp\{-nB(\alpha^*)\} \tag{25}$$

where α^*, the "optimal" micellar composition, is the composition for which $B(\alpha)$ in eq 20 is minimal. We can further simplify eq 24 by subtracting from it eq 23 multiplied by α^*. This yields

$$X(\alpha_s - \alpha^*) = X_1(\alpha_1 - \alpha^*) \tag{26}$$

which establishes a useful relation between the optimal composition of the micelles α^*, the composition of the free monomers α_1 and the overall composition of dissolved surfactant α_s.

It is noteworthy that eqs 23 and 25 are identical in structure to the mass-conservation relation, eq 12, and the micellar distribution, eq 14, found for the single-component micelles, with effective parameters evaluated at the optimal micellar composition α^*. In other words, we have demonstrated how the problem involving mixed micelles reduces to an effective one-component problem, as had been suggested earlier using a different approach.[13] This is an important result, since all the conclusions of Missel *et al.*[23] then follow immediately. Of these conclusions, we remark specifically that, in the limit of strong micellar growth ($X_1 e^{-B(\alpha^*)}$ close to unity), the weight-average micellar aggregation number $\bar{n}_w$ is given by

$$\bar{n}_w \simeq n_0 + 2\sqrt{K(\alpha^*)X} \tag{27}$$

It should be noted that, in contrast with the single-surfactant case, in a theory which derives the mixed micellar distribution starting from the chemical potentials, the correct normalizing prefactor in eq 16 does not appear naturally. This prefactor, $[2\pi n\alpha(1-\alpha)]^{-1/2}$, provides a correct reduction of eq 16 to the distribution function of single-component micelles, eq 11, in the case of $\epsilon(n,\alpha)$ independent of α (identical surfactants). Generally, for the S-component mixture, this prefactor should contain an extra $(2\pi n\alpha_s)^{-1/2}$ per each $S-1$ additional component, where α_s is the relative content of the s-th component in the mixture. Failure to take this into account will result in an extra $n^{(S-1)/2}$ factor in eq 25 arising from the saddle-point integration over all the α_s values. This will automatically lead to the conclusion that the average size of mixed micelles is proportional to $X^{2/(S+3)}$. Clearly, this conclusion is incorrect. For example, the size distribution of micelles is not affected by isotopic variability of the constituent surfactant molecules. In fact, $\bar{n}_w$ always scales like the square root of the total surfactant concentration,[13] exactly as in the single-component case, and not like $X^{2/5}$, as found by others[11] for the two-component mixture, $S = 2$.

IV. Experimental Results and Discussion

Combined QLS and Total Intensity Measurements: Examination of Micellar Shape. As stated in the Introduction, micelles of both pure $C_{12}E_6$ and pure $C_{12}E_8$ exhibit one-dimensional growth, albeit to different

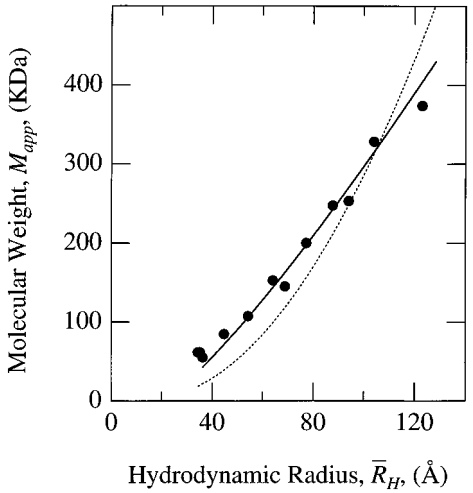

Figure 3. Apparent micelle molecular weight M_{app} plotted versus the average micelle hydrodynamic radius $\bar{R}_H$ for a mixture of $C_{12}E_6$ and $C_{12}E_8$ with solution composition $\alpha_s = 0.751$. The solid line is the prediction for a prolate ellipsoid with a semiminor axis $a = 3.4$ nm (the minimum radius measured). The dashed line is the prediction for an oblate ellipsoid with a semiminor axis $a = 3.4$ nm.

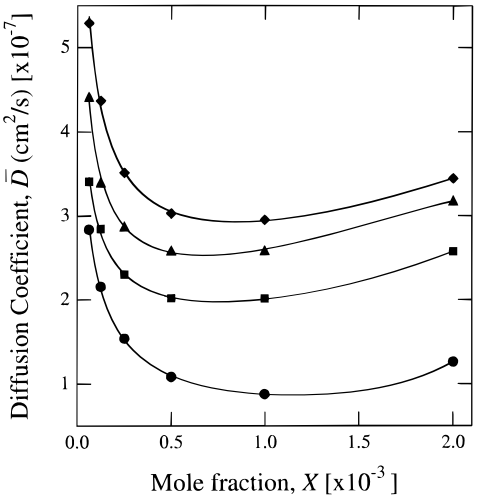

Figure 4. Average diffusion coefficient $\bar{D}$ measured as a function of total surfactant mole fraction X for an aqueous mixture of $C_{12}E_6$ and $C_{12}E_8$ with solution composition $\alpha_s = 0.848$: (circle) $T = 55$ °C; (square) $T = 50$ °C; (triangle) $T = 45$ °C; (diamond) $T = 40$ °C. The solid curves through the data points are guides to the eye.

extents. It would therefore be reasonable to assume that mixed micelles of $C_{12}E_6$ and $C_{12}E_8$ also grow in one dimension. We wish to confirm here that this is indeed the case and to investigate how the fact that micelles consist of two types of surfactant molecules affects the size distribution of micelles.

We determined the shape of the micelles by comparing data obtained by QLS with results derived from total intensity measurements. QLS experiments enable the determination of the diffusion coefficient of micelles in a sample solution. In the absence of strong intermicellar interactions, we can utilize eq 5 to calculate the average hydrodynamic radius of the micelles. In addition, extrapolation of the total intensity of the scattered light measured at different angles to zero angle allows us to determine the apparent molecular weight of the micelles. Since the molecular weight of the micelle is determined only by the numbers and types of surfactant molecules in it, while the hydrodynamic radius also depends on micelle shape, one can compare these two quantities to obtain information on the micellar configuration. As temperature and overall surfactant concentration change, the micelles can vary both in shape and in size. By plotting the apparent molecular weight versus the measured average hydrodynamic radius for micelles under different solution conditions, one can then distinguish between different models of micellar growth.

Combined QLS and total intensity measurements were performed on an aqueous mixture of $C_{12}E_6$ and $C_{12}E_8$ with solution composition $\alpha_s = 0.751$. We found that for this composition $dn/dc = 0.12 \pm 0.01$ cm^3/g. We determined the size and the molecular weight of micelles in three samples with total surfactant mole fractions well above the cmc: $X = 1.0 \times 10^{-4}$, 2.0×10^{-4}, and 3.3×10^{-4}, each at four temperatures $T = 25$, 35, 40, and 45 °C. In Figure 3, we plot as solid circles the apparent molecular weight of micelles M_{app} versus their average hydrodynamic radius $\bar{R}_H$ found in all these experiments. We see that M_{app} and $\bar{R}_H$ are nearly in direct proportion to each other, as is expected for the rodlike, spherocylindrical shape of the micelles. The hydrodynamic properties of such particles could be adequately approximated[52] by those of prolate ellipsoids with an appropriate semiminor radius a. We took $a = 3.4$ nm, which corresponds to the minimal size of the micelle obtained by an extrapolation of the measured hydrodynamic radius to zero concentration at 25 °C. Note that the total intensity measurements at the lowest concentration yield a molecular weight of 62 kDa, or approximately 135 monomers, a value which agrees with previous estimations of the molecular weight of the minimal micelles.[28] We took the density of the micelles to be a size-independent adjustable parameter. The solid curve in Figure 3 was calculated using eq 6 to determine the volume of an ellipsoid with a given R_H and using a density of 0.25 g/mL to calculate the molecular weight of this ellipsoid. Such a density of surfactants inside a micelle corresponds to an average micellar hydration of approximately 13 water molecules per ethylene oxide group. This value provides the best fit to the experimental data. For comparison, in Figure 3, we also plot the theoretical prediction for an alternative model of discoidal micellar growth. The dashed curve represents the best fit to the experimental data of the molecular weight versus hydrodynamic radius dependency for oblate ellipsoids with the same semiminor radius $a = 3.4$ nm. Clearly, the prolate ellipsoidal model fits the data significantly better, and we therefore conclude that, as expected, mixed micelles of $C_{12}E_6$ and $C_{12}E_8$ grow in one dimension.

QLS Measurements: Study of Micelle Sizes. QLS measurements were performed on solutions containing pure $C_{12}E_6$ and water ($\alpha_s = 1$), on solutions containing pure $C_{12}E_8$ and water ($\alpha_s = 0$), and on three different aqueous mixtures ($\alpha_s = 0.501$, 0.763, and 0.848) of $C_{12}E_6$ and $C_{12}E_8$. In Figure 4, we show the representative results of our measurements of the average diffusion coefficient $\bar{D}$, as a function of total surfactant mole fraction X. The data presented refer to a mixture of $C_{12}E_6$ and $C_{12}E_8$ with solution composition $\alpha_s = 0.848$ at temperatures of 40, 45, 50, and 55 °C. We observe that, for total surfactant concentrations above the cmc ($(2.0 \pm 0.10) \times 10^{-6}$) but still significantly less then the critical concentration for phase separation (between 9.4×10^{-4} for pure $C_{12}E_6$ and 1.1×10^{-3} for pure $C_{12}E_8$), the diffusion coefficient drops steeply as the surfactant concentration increases. This decrease in the diffusion coefficient reflects the growth of the micelles average hydrodynamic radius as concentration increases and is consistent with the predictions of

(52) de la Torre, J. G.; Bloomfield, V. A. *Q. Rev. Biophys.* **1981**, *14*, 81.

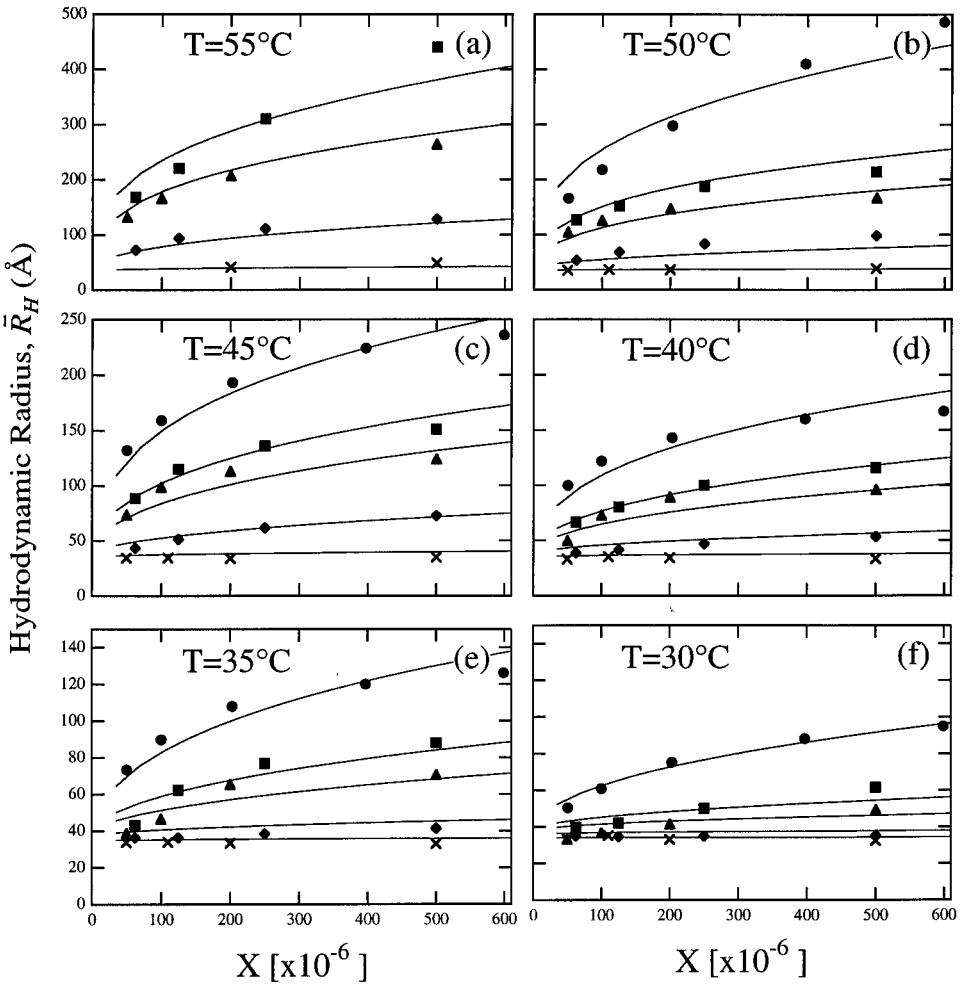

Figure 5. Average micelle hydrodynamic radius $\bar{R}_H$ measured as a function of total surfactant mole fraction X for aqueous mixtures of $C_{12}E_6$ and $C_{12}E_8$. The different symbols represent the different compositions studied: (cross) $\alpha_s = 0$ (pure $C_{12}E_8$); (diamond) $\alpha_s = 0.501$; (triangle) $\alpha_s = 0.763$; (square) $\alpha_s = 0.848$; (circle) $\alpha_s = 1$ (pure $C_{12}E_6$). Each panel contains measurements at the temperature indicated: (a) $T = 55$ °C; (b) $T = 50$ °C; (c) $T = 45$ °C; (d) $T = 40$ °C; (e) $T = 35$ °C; (f) $T = 30$ °C. The various curves are fits to the two-dimensional ladder model.

the ladder model. In addition, the diffusion coefficient decreases significantly as temperature increases. The viscosity of water decreases with temperature, and according to the Stokes−Einstein relation, eq 5, the diffusion coefficient normally increases with temperature. Therefore, the experimentally observed dependence of $\bar{D}(T)$ should be attributed to the growth of the micelles, caused by the temperature dependence of the growth parameters $\Delta\mu_A$ and $\Delta\mu_B$.

Figure 4 also indicates that, at all the temperatures examined, there is a minimum in the observed diffusivity plotted as a function of surfactant concentration. This minimum occurs in the vicinity of the critical concentration X_C for the phase separation of the micellar solution[14] and becomes relatively deeper as the temperature is increased toward the phase boundary. The presence of such a minimum has been observed previously in pure $C_{12}E_6$ solutions,[53] and two possible explanations of the phenomenon have been suggested. The first explanation[25,26,29−32] is based on the supposition that the same attractive interactions between micelles that cause phase separation also slow down the dissipation of the fluctuations in local concentration of the micelles. This is equivalent to a reduction in the collective diffusivity, which is measured in the QLS experiment. This concept connects the observed minimum in the diffusion coefficient to the proximity of the phase separation boundary, which qualitatively explains the position of the minimum near X_C, as well as the fact that the relative depth of the minimum increases when the temperature approaches the phase separation temperature. An alternative explanation that has been suggested recently[53] utilizes the analogy between a solution of long wormlike micelles and a semidilute polymer solution. This theory ascribes the growth in apparent diffusivity observed above a certain surfactant concentration to a transition from the individual diffusion of micelles to the collective motion of a micelle network formed in a semidilute solution of long entangled micelles. The position of the minimum in the apparent diffusion coefficient is then identified as a threshold between dilute and semidilute regimes in the micellar solution. Both these theories allow only qualitative analysis of our QLS data for the solutions with surfactant concentrations approaching X_C. Since in this work we are interested mostly in the thermodynamics of micellar growth, we restrict our subsequent attention to the regions of low surfactant concentration, well below $X = 1 \times 10^{-3}$, where our data can be unambiguously interpreted without bringing into consideration either intermicellar interactions or the entanglement of micelles.

Our main experimental results in this low surfactant concentration domain are displayed in Figure 5. Here we have plotted the average hydrodynamic radius of the mixed micelles, $\bar{R}_H$, at all the compositions (various symbols)

(53) Carale, T. R.; Blankschtein, D. *J. Chem. Phys.* **1992**, *96*, 459.

and temperatures (various panels) studied, as a function of surfactant concentration X. Figure 5 shows that the extent of micellar growth varies monotonically with the surfactant composition from unobservable (pure $C_{12}E_8$, crosses) to very significant (pure $C_{12}E_6$, circles). The extent of micellar growth also increases dramatically as the temperature undergoes a relatively small change from 30 °C (Figure 5f) to 55 °C (Figure 5a). We can now use the generalized "two-dimensional" ladder model described in the previous section to analyze the concentration, composition, and temperature dependence of the average micellar size in the mixed $C_{12}E_6$−$C_{12}E_8$ water system in the region of the phase diagram where the interactions between micelles can be neglected.

Comparison with Ladder Model Predictions and Analysis of the Free Energy of Micellization. Several parameters should be known to calculate theoretically the average hydrodynamic radius of the mixed micelles at given solution conditions. The first set of thermodynamic parameters includes the growth parameters $\Delta\mu_A$ and $\Delta\mu_B$, the micellization free energies associated with the minimal size micelles, Δ_A and Δ_B, and the aggregation number of the minimal size micelle, n_0. These five parameters fully describe the distribution of mixed micelles in a solution of any given concentration and composition of surfactants. Since at low surfactant concentrations, near the cmc, all micelles are very close in size to that of the minimal one, the critical micellar concentration measurements provide information only on the parameters Δ_A and Δ_B. The growth parameters $\Delta\mu_A$ and $\Delta\mu_B$, on the other hand, are responsible for the asymptotic size of the micelles at high surfactant concentrations (see eq 27) and, therefore, can be determined from the QLS measurements.

A set of structural parameters is needed to calculate the hydrodynamic radius of a micelle containing a certain number of surfactant monomers. As we have stated earlier, we model the micelle hydrodynamically as an effective prolate ellipsoid. The minor axis of this ellipsoid is always taken to be $a = 3.4$ nm, which is the minimum radius measured for the micelles. The major axis of the ellipsoid is assumed to increase with the number of surfactant molecules in the micelle in such a way as to provide a constant micellar density equal to 0.25 g/mL, in accordance with the total intensity measurements. The aggregation number of the minimal size micelle is taken to be $n_0 = 135$. This number was also determined from total intensity measurements and agrees well with previous estimations.[28] The average hydrodynamic radius was then calculated using eq 6 and the distribution function given by eq 25. The contribution from each micellar species was weighted according to its scattering amplitude determined by the mass of the micelle and an appropriate form factor. The micellization free energies Δ_A and Δ_B were taken to provide cmc values equal to 2.0×10^{-6}, whereas the growth parameters $\Delta\mu_A$ and $\Delta\mu_B$ of the two-dimensional ladder model in eq 18 were treated as adjustable parameters. The precise details of this procedure have been described elsewhere.[44]

The predictions of the model with the optimal choice of the parameters, shown in Figure 5 as the solid curves, are in very good agreement with the experimental data. As can be seen, two adjustable parameters, $\Delta\mu_A$ and $\Delta\mu_B$, that we determined for each temperature, are sufficient to successfully describe the growth of mixed micelles of every composition studied from pure $C_{12}E_8$ (crosses) to pure $C_{12}E_6$ (circles). The values of the parameters $\Delta\mu_A$ and $\Delta\mu_B$ that yield the best fit to the experimental data at each temperature are shown in Figure 6. Note that the growth parameters can be accurately determined only for the samples that exhibit significant micellar growth. Since the extent of this growth correlates with the proportion of $C_{12}E_6$ (surfactant A) in the solution, the deduced values of $\Delta\mu_A$ are more accurate than those of $\Delta\mu_B$. Nevertheless, even for $\Delta\mu_B$, we did obtain a consistent set of values that systematically vary with temperature. This implies that the two-dimensional ladder model provides an adequate phenomenological description of dilute aqueous solutions of the $C_{12}E_6$−$C_{12}E_8$ surfactant mixture.

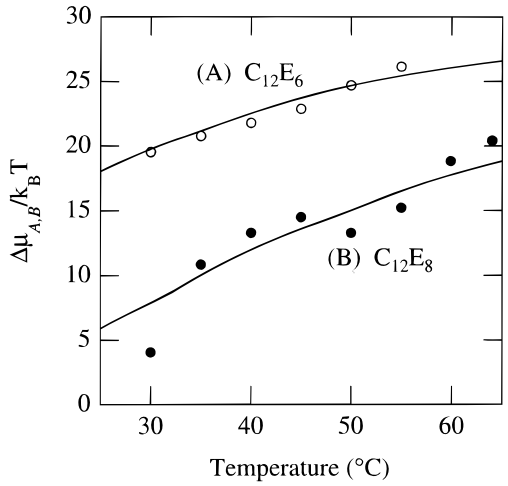

Figure 6. Two-dimensional ladder model growth parameters, $\Delta\mu_A/k_BT$ (open circles, A) and $\Delta\mu_B/k_BT$ (closed circles, B), for the $C_{12}E_6$−$C_{12}E_8$ water system plotted as a function of temperature. These parameters (except for the values above $T = 55$ °C) were deduced from the data of Figure 5. The values of $\Delta\mu_B/k_BT$ for $T > 55$ °C were obtained from additional measurements on $C_{12}E_8$ not shown in Figure 5.[44] The solid curves are the predictions of the molecular−thermodynamic model of Puvvada and Blankschtein.[13,14]

In our theoretical analysis, specifically, in deriving eq 16, we assumed that the composition of the central cylindrical part of the micelle is the same as the composition of the end caps. It can be shown that this assumption is valid in the limit $(\Delta\mu_A - \Delta\mu_B)/n_0 \ll k_BT$. In the case of similar surfactants like $C_{12}E_6$ and $C_{12}E_8$ one might expect that this condition is fulfilled. Indeed, this turns out to be the case according to the data shown in Figure 6. However, as is clear from eq 18, the dependence of the micelle distribution on composition itself is caused by the difference between $\Delta\mu_A$ and $\Delta\mu_B$. Therefore, in a rigorous analysis, the difference in compositions between the end caps and the cylindrical body of the micelle may not be neglected. We performed such a rigorous analysis and found that[44] (i) eq 25 still holds in this case with a slight redefinition of the quantities $K(\alpha^*)$ and $B(\alpha^*)$ and (ii) the numerical values of the growth parameters that provide the best fit to the experimental data remain the same within the experimental uncertainty. For these reasons, we decided to present here only the simplified version of the theoretical treatment.

We will next focus our attention on the analysis of the magnitude and temperature dependence of the phenomenological growth parameters, $\Delta\mu_A$ and $\Delta\mu_B$, shown in Figure 6, from a microscopic, molecular−thermodynamic viewpoint. The theoretical framework for such an analysis has been recently developed in a series of papers by Puvvada and Blankschtein.[13,14] In this approach, the free energy of micellization is interpreted as a sum of five different contributions: (1) the transfer of the surfactant hydrophobic tails from water to a bulk hydrocarbon environment, (2) the creation and partial screening of the micellar core−water interface, (3) the loss of entropy associated with restricting the configurations of the

hydrophobic tails in the micellar core, (4) the steric repulsions between the hydrophilic head groups at the micellar core−water interface, and (5) electrostatic interactions between the hydrophilic head groups in the case of charged surfactants. Of these contributions, all but the steric free energy contribution have been estimated using readily available information about the surfactant species involved in the micellization process.[14]

The steric free energy contribution to the total free energy of micellization results from steric repulsions between the hydrophilic head groups at the surface of the micelle. This contribution has an entropic nature and originates from the reduction in the number of possible configurations available to an additional head group due to the presence of head groups of other surfactant molecules at the micellar surface. Assuming that the concentration of head groups at the micelle surface is sufficiently low so that their excluded volumes may be considered in an additive fashion, the steric contribution to the micellization free energy, g_{st}, can be modeled as[14]

$$g_{st} = -k_B T \ln\left[1 - \frac{\alpha a_{hA} + (1-\alpha) a_{hB}}{a}\right] \qquad (28)$$

where a_{hA} is the average cross-sectional area of a surfactant A head group, a_{hB} is the average cross-sectional area of a surfactant B head group, and a is the total area at the micellar surface per surfactant molecule. It is further assumed that the average cross-sectional area a_{hj} of C_iE_j surfactants depends only on the number j of ethylene oxide groups in the molecule and on the degree of hydration of these groups. Since the extent of hydration should decrease with temperature, the temperature dependence of a_{hj} has been modeled using the following simple linear relation:[49]

$$a_{hj} = a^\circ_{hj}[1 - H_j(T - 298)] \qquad (29)$$

where a°_{hj} is the value of a_{hj} at 298 K and H_j reflects the reduction of a_{hj} with temperature. With these assumptions, Puvvada and Blankschtein[14] were able to produce a computational scheme that predicts the micellization free energy from molecular characteristics of nonionic surfactants. Conversely, this scheme allows one to reconstruct, from the experimentally measured temperature dependence of the micellization free energy, the important molecular parameters a_{hj} and H_j.

A simplified version of this molecular−thermodynamic model, considering only solutions containing a single surfactant species, was previously applied to the analysis of the $C_{12}E_6$−water system.[49] It was found that, for $C_{12}E_6$, $a^\circ_{h6} = 38.1$ Å^2 and $H_6 = 0.0075$ K^{-1}. The value for H_6 was determined by fitting the experimentally observed temperature dependence of the critical micellar concentration of $C_{12}E_6$. Considering that this dependence is extremely weak, the parameter H_6 could hardly be determined with great accuracy using this method. Until our work, only the information on the micellization free energy of pure $C_{12}E_6$ aqueous solutions has been available. In order to estimate the value of a_{hj} for other surfactants in the C_iE_j family, Puvvada and Blankschtein[49] suggested that the temperature dependence of this quantity should be the same across the entire family and that, at any given temperature, it should vary with the hydrophilic head group length j as $a_{hj} \sim j^{0.8}$. Accordingly, for $C_{12}E_8$, $a^\circ_{h8} = 38.1 \times (8/6)^{0.8} = 48.0$ Å^2 and $H_8 = 0.0075$ K^{-1}. We have used this molecular−thermodynamic theory to fit the values of the growth parameters $\Delta\mu_A$ and $\Delta\mu_B$ that we deduced from our measurements. The parameters a°_{hj} and H_j listed in Table 1 gave the best fit to our data, as shown by the solid lines in Figure 6. These values of a°_{hj} and H_j should be viewed as an improvement over the previous estimates.[14] It appears that the a_{h8} value, originally estimated using a scaling argument,[49] is higher than the actual value shown in Table 1. In addition, the deduced H_8 value is slightly smaller than H_6, implying a weaker dehydration of the $C_{12}E_8$ hydrophilic heads with increasing temperature, as compared to that of the $C_{12}E_6$ hydrophilic heads.

Table 1. Estimates of a°_{hj} and H_j for $C_{12}E_6$ and $C_{12}E_8$

	a°_{hj} (Å^2)	H_j (K^{-1})
$C_{12}E_6$	38.8	0.007 25
$C_{12}E_8$	44.9	0.005 59

V. Conclusions

We studied the growth of mixed micelles composed of $C_{12}E_6$ and $C_{12}E_8$ using static and quasielastic light scattering. By comparing the measured values of the apparent molecular weight and the average diffusion coefficient of micelles, we have shown that the mixed micelles grow in one dimension. We generalized the ladder model to the case of mixed micelles and demonstrated how the description of the mixed system reduces to the description of the pure system by utilizing composition-dependent model parameters. We measured the average diffusion coefficient $\bar{D}$ of the micelles as a function of total surfactant concentration in the temperature range 10 °C $\leq T \leq$ 55 °C for aqueous solutions of pure $C_{12}E_6$, pure $C_{12}E_8$, and three different mixtures of $C_{12}E_6$ and $C_{12}E_8$. All of these data have been successfully explained in terms of our "two-dimensional" generalization of the ladder model in the regions of the phase diagram where the interactions between micelles are weak. The growth parameters of the generalized ladder model were deduced from our data. A microscopic theory was applied to calculate the conformational characteristics of both surfactants that correspond to the deduced values and temperature dependence of the growth parameters.

Acknowledgment. We thank Dr. Sudhakar Puvvada for many useful discussions. D.B. is grateful to Kodak, Uniliver, and Witco for providing partial support for this work. The work of H.G.T. was supported by the Opto-Radar Systems Group at MIT Lincoln Laboratory and by the MIT Center for Materials Science and Engineering under NSF Grant DMR 90-22933.

LA9606613